

Table 1 Comparison between analytical predictions and experimental results

	Case 1, $M_s = 1.25$, $\theta_w^1 = 55$ deg, $\theta_w^2 = 90$ deg		Case 2, $M_s = 1.49$, $\theta_w^1 = 55$ deg, $\theta_w^2 = 90$ deg	
	Analysis	Experiment	Analysis	Experiment
χ_1 , deg	57.6	52 deg ± 1	56.9	52 deg ± 1
χ_2 , deg	39.1	44 deg ± 1	34.7	37.5 deg ± 1
θ_m , deg	56.6	56 deg ± 1	58.4	58 deg ± 1

The set of 32 governing equations consists of the following 32 unknowns: v_C , M_{C1} , M_{C2} , $M_1(C)$, $M_2(C)$, $\beta_1(C)$, $\beta_2(C)$, $\delta_4(C)$, $\delta_6(C)$, $p_4(C)$, $p_6(C)$, M_m , θ_m , m_2 , $\phi_4(C)$, $\phi_6(C)$, χ_1 , v_D , M_{D1} , M_{D2} , $M_1(D)$, $M_3(D)$, $\beta_1(D)$, $\beta_3(D)$, $\delta_5(D)$, $\delta_6(D)$, $p_5(D)$, $p_6(D)$, m_3 , $\phi_5(D)$, $\phi_6(D)$ and χ_2 .

Note that the speed of sound a_1 behind the incident shock wave is simply obtained from M_s and a_0 . The parameters M_{i1} , θ_1 , a_2 , and ω_1 can be obtained from solving the regular reflection of incident shock wave M_s over the first reflecting surface θ_w^1 . Similarly, M_{i2} , θ_2 , a_3 , and ω_2 can be obtained from solving the regular reflection of the incident shock wave M_s over the second reflecting surface θ_w^2 . Recall that M_s , θ_w^1 , θ_w^2 , and the flow state (0) are all known, as they are the initial conditions.

Results and Discussion

Predictions of the proposed analytical model were compared with the relevant experimental results of Refs. 1–3. Three geometrical parameters were compared: the first and second triple point trajectory angles χ_1 and χ_2 and the orientation of the Mach stem θ_m with respect to the horizontal x axis. The comparison is shown in Table 1. Whereas the analytical predictions of χ_1 overestimate the experimental results by about 10%, the analytical predictions of χ_2 underestimate the experimental results by about 10%. Although these agreements do not seem to be too good, one should recall that similar agreement is obtained when the three-shock theory is used to predict the triple-point trajectory angle in Mach reflections over single wedges.⁴ The reason for this disagreement lies in the fact that in actual triple points not all of the shock waves are straight as required by the two- and three-shock theories. Figures 2a and 2b clearly indicate this fact. Furthermore, whereas in the case of single wedges the triple point moves toward a quiescent gas in the wave configuration treated in the present study, the triple points move toward a moving gas. Consequently, the present problem is much more complicated and, hence, an agreement within 10% should practically be considered as a very good one. Finally, it should be noted that as is evident from Table 1, the agreement between the presently proposed analytical model and the experimental results, regarding the orientation of the Mach stem, i.e., θ_m , is excellent.

Conclusions

The two- and three-shock theories were applied to complex flow-fields and wave structures. Their performance was found to be good to excellent. By further developing this model the pressures acting on the surfaces can be estimated.

References

- Ben-Dor, G., Dewey, J. M., and Takayama, K., "The Reflection of a Plane Shock Wave Over a Double Wedge," *Journal of Fluid Mechanics*, Vol. 176, 1987, pp. 483–520.
- Itoh, K., Takayama, K., and Ben-Dor, G., "Numerical Simulation of the Reflection of a Planar Shock Wave Over a Double Wedge," *International Journal of Numerical Methods in Fluids*, Vol. 13, 1991, pp. 1153–1170.
- Falcovitz, J., Alfandary, G., and Ben-Dor, G., "Numerical Simulation of the Head-On Reflection of a Regular Reflection," *International Journal of Numerical Methods in Fluids*, Vol. 17, 1993, pp. 1055–1078.
- Ben-Dor, G., *Shock Wave Reflection Phenomena*, Springer-Verlag, New York, 1991, Chap. 1.

Effect of Screen Porosity and Location on Wind-Tunnel Turbulence

G. Refai Ahmed* and E. Brundrett†

University of Waterloo,
Waterloo, Ontario N2L 3G1, Canada

Introduction

ONE of the fundamental problems of engineering fluid mechanics is how to control the velocity distribution of fluid flow inside the wind tunnel. Often, single screen or multiple screens are used in this operational mode to remove or create time-mean velocity nonuniformities and to reduce or increase the intensity of turbulence in a controlled manner. Numerous studies have investigated the effect of placing screens in the fluid flow through wind tunnels since the beginning of this century. Furthermore, the researchers have examined the effect of the turbulence intensity, as controlled by the screens, on forced convection heat transfer results.

A wide variety of turbulence generators have been examined in the past, such as square-mesh arrays of either round rods or wires (woven screens), square-mesh arrays of square bars, parallel arrays of square bars, perforated plates, agitated bar grids, jet grids, aerofoil cascades, tube bundles, and various permutations and combinations of the preceding. Roach¹ investigated the pressure drop across screens and the characteristics of the downstream turbulence. Furthermore, Roach¹ attempted to fill gaps in the current literature by proposing simple rules for the design of screens in wind tunnels. Therefore, he proposed design guidelines and also examined the pressure losses, turbulence intensities, spectra, correlation functions and length scales. In addition, Roach¹ introduced a number of correlations to predict turbulence intensity behind a screen; however, he did not address the effect of screen porosity on turbulence intensity. Laws and Livesey² investigated the flow through screens by characterizing the flow properties of the screen, by determining the effect of a screen on time-mean velocity distributions, and by measuring the turbulence distribution downstream of gauze screens. Furthermore, Gad-el-Hak and Corrsin³ gave details of turbulence intensities, scales, decays, and spectra for their jet grid. In the same paper they summarized the results, in tabular form, of no less than 12 previous paper on both passive and active grids giving the turbulence component magnitudes and decays of the form

$$\cot u/u \times 100Tu = B(x/M)^{-m} \quad (1)$$

where B and m are constants, x is the distance between the location of the screen and the measurement location of Tu , and M is square cell width of the screen based on wire centerline. Batchelor and Townsend⁴ and Compte-Bellot and Corrsin⁵ correlated their

Received April 4, 1994; revision received Sept. 15, 1994; accepted for publication Sept. 20, 1994. Copyright © 1994 by the American Institute of Aeronautics and Astronautics, Inc. All rights reserved.

*Graduate Research Assistant, Department of Mechanical Engineering, Senior Member AIAA.

†Professor, Department of Mechanical Engineering.

experimental data in the following form:

$$Tu = b \left(\frac{x}{M} - \frac{x_0}{M} \right)^{-n} \quad (2)$$

where b and n are constants which depend on the screen dimensions, and x_0 introduces a virtual origin to the correlation.

Nonetheless one can still find some limitations in Eqs. (1) and (2), such as both the screen porosity and Reynolds number effects on the turbulence intensity ($Re_d = dU/\nu$), which are, however, well recognized in pressure loss correlations of screens (see Brundrett⁶). Therefore, the main objectives of the present study can be summarized as follows.

- 1) Study the effect of different woven screens on the turbulence intensity of the downstream flow.
- 2) Investigate the effect of Reynolds number on turbulence intensity and, if necessary, limit the recommended correlation to an appropriate range of Reynolds numbers.
- 3) Examine the variation of turbulence intensity with downstream distance from the screen.
- 4) Develop a general model to predict turbulence intensity for a practical wind-tunnel range.

Analysis of Currently Available Screen Data

Kestin et al.⁷ conducted a series of experiments to investigate the influence of turbulence on the heat transfer from plates using a screen with wire spacing $M = 0.019$ m and wire diameter $d = 0.003759$ m at a distance $x = 0.47$ m upstream of the testing object. By examining the Kestin et al.⁷ measurements it can be shown that there is data scatter and a significant variation of Tu with increasing Reynolds number. In contrast, measurements by both Raithby⁸ and Boulos⁹ show no significant variation of Tu with increasing Re_d in the range $200 < Re_d < 3000$. In addition, the trends of Tu vs x have a power-law form which also shows in the correlation (Table 1) of the data of Raithby,⁸ Boulos,⁹ and Tan-Atichat et al.¹⁰ Figure 1 shows the relationships between turbulence intensity and screen location in dimensionless form x/M for different screen porosities a (defined as fraction open area) where $0.55 < a < 0.77$. Roach¹ proposed a single correlation to model the data in order to predict the average Tu at any x/M . However, this approach neglected porosity, with all data in the range of $0.55 \leq a \leq 0.65$ and, therefore, is not sufficiently general for all turbulence modifying screen applications.

The present investigation examines the data of Smith and Kuethe,¹¹ Raithby,⁸ Boulos,⁹ and Tan-Atichat et al.¹⁰ Their turbulence intensity experimental data are all dependent on screen porosity, Reynolds number, and the dimensionless distance downstream of the screen x/M . The present study proposes the following general correlation for these experimental data as follows:

$$Tu = \left[\frac{0.428}{a(x/M)^{0.4}} \right]^2 \quad (3)$$

where, for woven screens practical ranges for screen porosities and Reynolds number are

$$0.5 \leq a \leq 0.8$$

$$200 < Re_d < 3000$$

Furthermore, it is proposed that the minimum and maximum values of x/M are

$$\left(\frac{x}{M} \right)_{\text{minimum}} = \frac{6.7}{a^{2.5}} \quad (4)$$

$$\left(\frac{x}{M} \right)_{\text{maximum}} = \frac{90}{a^{2.5}} \quad (5)$$

where Tu changes too rapidly with x/M below the minimum limit to be practical and becomes nearly asymptotic for x/M above the maximum limit. One can observe from Eq. (3) that Tu is proportional to $1/a^2$, however, ΔP is proportional to $(1 - a^2)/a^2$ as concluded

Table 1 Previous correlations of $Tu = A(x/M - x_0/M)^{-n}$

Author	a	M	A	x_0/M	n
Raithby ⁸	0.56	0.0254	0.314	3.0	0.645
	0.661	0.0191	0.203	6.0	0.633
	0.765	0.0127	0.168	9.0	0.686
Boulos ⁹	0.60	0.00317	0.099	21.9	0.5
	0.64	0.0102	0.103	8.4	0.46
Tan-Atichat et al. ¹⁰	0.554		0.174	0.0	0.5

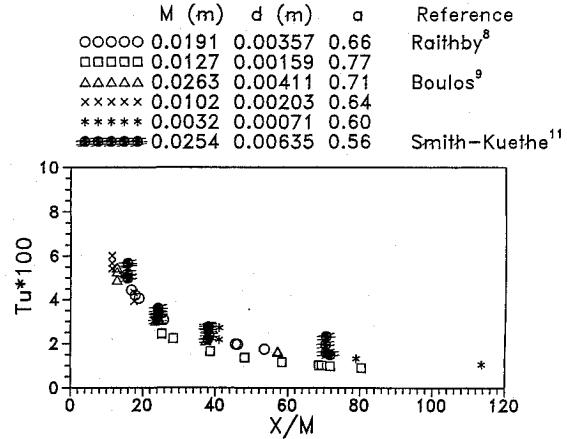


Fig. 1 Effect of a on the relationship between Tu and x/M .

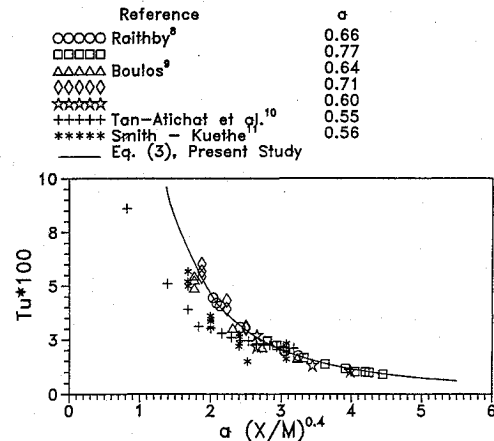


Fig. 2 Comparison between the present model, Eq. (3) and the previous experimental studies.

by Brundrett.⁶ Furthermore, Roach¹ found that Tu is proportional to $(x/M)^{-5/7}$, however, the present study found that the best fit can be obtained at $(x/M)^{-0.8}$. In contrast to Eq. (3), Raithby,⁸ Boulos,⁹ and Tan-Atichat et al.¹⁰ proposed a group of correlations for their experimental data, as shown in Table 1. These correlations could not be used below the reporting values of x_0/M in Table 1 since they do not estimate the experimental values of Tu at x_0/M . Furthermore, Groth and Johansson¹¹ presented various relationships of Tu and x/M in the range of $0.56 \leq a \leq 0.71$ and $13 \leq Re_d \leq 830$. One can observe, from their study, that the values of Tu corresponding to $a = 0.71$ are greater than values of Tu corresponding to $a = 0.63$ or $a = 0.58$ at fixed x/M , for $x/M > 25$. In addition, in the range of $x/M < 25$, the values of Tu at fixed x/M for screens with $a = 0.61$ and $a = 0.71$ are also greater than those for a screen with $a = 0.65$.

Furthermore, Fig. 2 shows a comparison between the proposed model, Eq. (3), and the previous experimental data of Raithby,⁸ Boulos,⁹ Tan-Atichat et al.,¹⁰ and Smith and Kuethe.¹² It can be seen that there is very good agreement between the present model Eq. (3) and both Boulos⁹ and Raithby⁸ in their reported data ranges. In contrast, the data of Tan-Atichat et al.¹⁰ are smaller than the predication of Eq. (3) in the range of $0.8 \leq a(x/M)^{0.4} \leq 2.5$ by

68–14%. After that, their data have good agreement with Eq. (3). Also, Eq. (3) is greater than the data of Smith and Kuethe¹² [the maximum difference is 21% at $a(x/M)^{0.4} = 2$]. Equation (3) shows that the freestream turbulence can increase by 49%, when the porosity changes from 0.55 to 0.77.

One of the applications of this investigation is external forced convection heat transfer from a body shape inside a wind tunnel. Consider a flat plate with length L behind a woven screen with mesh spacing M . The leading edge of the flat plate is at x_a from the screen, and the end is at x_b , $x_b = x_a + L$. The Tu at both x_a and x_b can be determined from Eq. (3) and will show a decrease in Tu along the plate. It is recommended that the best value of Tu for heat transfer along the flat plate or other body shapes can be estimated using the harmonic average value of Tu , i.e.,

$$Tu = \sqrt{Tu_{x_a} \cdot Tu_{x_b}} \quad (6)$$

Summary and Conclusions

The effect of screens on wind-tunnel turbulence was examined in this study from different aspects, such as the effect of Reynolds number, screen porosity, and screen location. Furthermore, the present study developed a model to predict the turbulence intensity, based on experimental data, as a function of porosity and downstream distance. Also, this investigation found that there is no significant effect of Re_d on Tu , for the practical wind-tunnel range of $200 < Re_d < 3000$.

Acknowledgments

The second author acknowledges the financial support of the Natural Sciences and Engineering Research Council of Canada under Grant University of Waterloo 6078. The authors wish to thank M. M. Yovanovich of the University of Waterloo, Ontario, and F. Spaid at McDonnell Douglas Aerospace, St. Louis, Missouri, for their valuable discussions.

References

- Roach, P. E., "The Generation of Nearly Isotropic Turbulence by Means of Grids," *International Journal of Heat and Fluid Flow*, Vol. 8, No. 1, 1987, pp. 82–92.
- Laws, E. M., and Livesey, J. L., "Flow Through Screens," *Annual Review of Fluid Mechanics*, Vol. 10, 1978, pp. 247–266.
- Gad-el-Hak, M., and Corrsin, M., "Measurements of the Nearly Isotropic Turbulence Behind a Uniform Jet Grid," *Journal of Fluid Mechanics*, Vol. 62, 1974, pp. 115–143.
- Batchelor, G. K., and Townsend, A. A., "Decay of Isotropic Turbulence in the Initial Period," *Proceedings of the Royal Society A*, Vol. 193, 1947, pp. 538–554.
- Comte-Bellot, G., and Corrsin, S., "The Use of a Contraction to Improve the Isotropy of Grid-Generated Turbulence," *Journal of Fluid Mechanics*, Vol. 25, 1966, pp. 657–662.
- Brundrett, E., "Prediction of Pressure Drop for Incompressible Flow Through Screens," *Journal of Fluids Engineering*, Vol. 115, No. 2, 1993, pp. 239–242.
- Kestin, J., Maeder, P. F., and Wang, H. E., "Influence of Turbulence on the Transfer of Heat from Plates with and without a Pressure Gradient," *International Journal of Heat and Mass Transfer*, Vol. 3, No. 1, 1961, pp. 133–154.
- Raithby, G., "The Effect of Turbulence and Support Position on the Heat Transfer from, and Flow Around, Spheres," Ph.D. Thesis, Univ. of Minnesota, 1967.
- Boulos, M., "Dynamics of Heat Transfer from Cylinders in a Turbulent Air Stream," Ph.D. Thesis, Dept. of Chemical Engineering, Univ. of Waterloo, Waterloo, ON, Canada, 1972.
- Tan-Aitchat, J., Nagib, H. M., and Loehrke, R. I., "Interaction of Free-Stream Turbulence with Screens and Grids: a Balance Between Turbulence Scales," *Journal of Fluid Mechanics*, Vol. 144, 1982, pp. 501–528.
- Groth, J., and Johansson, A. V., "Turbulence Reduction by Screens," *Journal of Fluid Mechanics*, Vol. 197, 1988, pp. 139–155.
- Smith, M. C., and Kuethe, A., "Effects of Turbulence on Laminar Skin Friction and Heat Transfer," *Physics of Fluids*, Vol. 9, No. 12, 1966, pp. 2337–2344.

Efficient Design Constraint Accounting for Mistuning Effects in Engine Rotors

Durbha V. Murthy*

University of Toledo, Toledo, Ohio 44135

and

Christophe Pierre† and Gísli Óttarsson‡

University of Michigan, Ann Arbor, Michigan 48109

Introduction

NEARLY all design and dynamic analysis procedures for engine blades are based on the assumption that all blades on a rotor are identical. This assumption of perfect cyclic symmetry is only approximately true in practice. Small differences in blade properties, commonly referred to as mistuning, are unavoidable because they arise from manufacturing tolerances and in-service degradation. The implicit assumption in most of the design procedures in that mistuning does not significantly affect the vibratory response of the blades.

That this assumption could be wrong has been demonstrated by several studies in which the influence of small levels of mistuning on blade assembly dynamics was investigated.¹ The adverse effects of mistuning on forced response can be drastic, possibly resulting in several hundred percent increases in the blade amplitudes. In such cases, the tuned rotor assumption gives highly misleading results. This sensitivity to mistuning can be particularly dangerous when automated design optimization procedures are employed. An optimal design that is extremely sensitive to mistuning may result, invalidating the optimization process.

An obvious approach to account for the effects of mistuning is to model a mistuned rotor and place constraints on blade amplitudes. However, it is then no longer sufficient to model a single blade, leading to large increases in analysis time. Also, the actual mistuning pattern is not available until the manufacture of the rotor is complete, and mistuning differs from rotor to rotor. Furthermore, the mistuning that results from in-service degradation cannot be modeled deterministically. Thus, even a full-scale mistuned analysis cannot be usefully performed in a deterministic manner.

In this Note, we suggest a way out of this impasse. Our approach is based on the realization that the tuned rotor assumption, in spite of its limitations, is valuable in analyses and optimization procedures because of the associated analytical simplifications and computational advantages. We present a strategy to develop a constraint that restricts the sensitivity of a design to mistuning. We illustrate the approach by applying it to a popular bladed-disk model. The proposed constraint is dependent on the properties of only the tuned system, so a mistuned system analysis is not needed. A statistical model of mistuning is chosen, and so no knowledge of the actual mistuning pattern is needed. The statistics of mistuning can be estimated for a population of manufactured rotors. In addition, the time-consuming mistuned system analysis is avoided by employing perturbation theory. The proposed constraint is also easy to differentiate provided a sensitivity analysis of the tuned assembly is available, making it suitable for the computation-intensive optimization of engine

Presented as Paper 92-4711 at the AIAA/USAF/NASA/OAI Symposium on Multidisciplinary Analysis and Optimization, Cleveland, OH, Sept. 21–23, 1992; received Oct. 22, 1993; revision received July 15, 1994; accepted for publication July 18, 1994. Copyright © 1994 by the authors. Published by the American Institute of Aeronautics and Astronautics, Inc., with permission.

*Senior Research Associate, Department of Mechanical Engineering; also Resident Research Associate, Structures Division, NASA Lewis Research Center. Senior Member AIAA.

†Associate Professor, Department of Mechanical Engineering and Applied Mechanics. Member AIAA.

‡Graduate Research Assistant, Department of Mechanical Engineering and Applied Mechanics. Member AIAA.